ANNALS OF GEOPHYSICS, 55, 1, 2012; doi: 10.4401/ag-5276

Special Issue: EARTHQUAKE PRECURSORS

Attenuation of electromagnetic waves at the frequency ~1.7 kHz in the upper ionosphere observed by the DEMETER satellite in the vicinity of earthquakes

David Píša[1,2,3], František Němec[2], Michel Parrot[1], Ondřej Santolík[3,2]

[1] *Laboratoire de Physique et Chimie de l'Environnement et de l'Espace, Université d'Orléans, CNRS, Orléans, France*

[2] *Charles University in Prague, Faculty of Mathematics and Physics, Prague, Czech Republic*

[3] *Institute of Atmospheric Physics, Academy of Science of the Czech Republic, Prague, Czech Republic*

Article history
Received July 7, 2011; accepted September 19, 2011.
Subject classification:
Surveys, measurements, and monitoring, Waves and wave analysis, Wave propagation.

ABSTRACT

The DEMETER satellite was the first satellite specifically dedicated to the recording of electromagnetic phenomena connected with seismic activity. Almost 6.5 years of measurements provide good opportunities to analyze a unique dataset with global Earth coverage. We present the results of a statistical study of the intensity of very low frequency electromagnetic waves recorded in the upper ionosphere. Robust two-step data processing has been used. The expected unperturbed distribution of the power spectral densities of electromagnetic emissions was calculated first. Then, the power spectral densities measured in the vicinities of earthquakes are compared with the unperturbed distribution and are examined for the presence of uncommon effects related to seismic activity. The statistical significance of the observed effects is evaluated. We confirm the previously reported results of a very small, but statistically significant, decrease in wave intensities a few hours before times of main shocks using this much larger dataset. The wave intensity decrease at a frequency of about 1.7 kHz is observed only during the night and only for shallow earthquakes. This can potentially be explained by increases in the cut-off frequency of the Earth ionosphere waveguide caused by imminent earthquakes.

1. Introduction

Over the past two decades, considerable progress has been made in the field of seismo-electromagnetic effects. The main aim of this study is to find possible short-term precursors of earthquakes that would allow us to predict these devastating events. Although various types of possible precursors have been reported (e.g. changes in temperature or conductivity), electromagnetic perturbations are probably one of the most promising candidates. These have been observed both using ground-based measurements and satellites, and they are believed to occur across a wide range of frequencies, from direct current to very high frequency [Parrot and Mogilevsky 1989, Larkina et al. 1989, Tate and Daily 1989, Serebryakova et al. 1992, Molchanov et al. 1993, Parrot 1994, Asada et al. 2001, Bortnik et al. 2008, Hobara et al. 2005, Němec et al. 2008, 2009]. However, it remains very difficult to identify these effects in the ionosphere, because they are most certainly particularly weak when compared to other electromagnetic effects due to other sources (e.g. lightning, geomagnetic storms, man-made noise). Consequently, there is still controversy concerning the actual existence of these seismo-electromagnetic effects, and there are quite a few studies that dispute their existence [Henderson et al. 1993, Rodger et al. 1996, Clilverd et al. 1999].

There are many theories that try to describe the processes before upcoming earthquakes and to explain why precursors should be observed; e.g. motion of the positive holes [Freund 2007, 2011], microfracturing electrification [Gershenzon et al. 1989, Molchanov and Hayakawa 1998, Molchanov et al. 2006], or a release of radon gas [Sorokin et al. 2001]. Nevertheless, widely accepted and demonstrated short-term precursors are still missing.

The advantage of the robust statistical study that we present here is that we are able to exclude the electromagnetic variations due to other than seismic sources. A similar statistical study that used a dataset obtained by the DEMETER (Detection of Electro-Magnetic Emissions Transmitted from Earthquake Regions) satellite was performed by Němec et al. [2008]. They systematically investigated 2.5 years of the DEMETER data, and they showed that during the night there was a small, but statistically significant, decrease in wave intensities in the vicinity of earthquakes shortly before (0-4 h) the time of the main shock.

In the present study, we applied the method of Němec et al. [2008] to the complete dataset acquired by DEMETER

(~6.5 years). The dataset that we used is described in Section 2. Section 3 presents the data processing method that we applied. The results that were obtained are presented in Section 4, and discussed in Section 5. Finally, Section 6 gives a brief summary.

2. The dataset

DEMETER was a low-altitude satellite (altitude, 710 km) that was launched in June 2004, on a circular polar orbit. It measured electromagnetic waves and plasma parameters all around the globe, except in the auroral zones [Parrot 2006]. The altitude of the satellite was decreased to 660 km in December 2005. The satellite science mission came to an end in December 2010, providing a total of about 6.5 years of data. The orbit of the DEMETER satellite was nearly Sun-synchronous. The up-going half-orbits corresponded to night-time (22.30 LT), whereas the down-going half-orbits corresponded to day-time (10.30 LT). The electric field measurements were carried out by an electric field instrument known as an ICE (Instrument Champ Electrique), which operated from direct current up to about 3 MHz. There were two different modes of operation of the satellite, called 'burst' and 'survey'. During the burst mode, more detailed data were collected. However, this was active only above limited areas, and therefore it is not very suitable for the intended statistical study. In the survey mode and the very low frequency (VLF) range (20 Hz to 20 kHz) that we have used, the frequency spectra of one electric field component calculated on board with a frequency resolution of about 19.5 Hz and a time resolution of either 2.048 s or 0.512 s are available. A more detailed description of the ICE instrument can be found in Berthelier et al. [2006].

We limited our analysis to the frequency range below 10 kHz, to avoid the frequencies of terrestrial VLF transmitters. Following Němec et al. [2008], we selected 16 frequency bands (117 Hz each) in such a way that they omit spacecraft interferences and cover the entire studied frequency range as uniformly as possible. We also limited our analysis to the geomagnetic latitudes between –65 and +65 degrees, because there were no data acquired by DEMETER at larger geomagnetic latitudes. All of the appropriate data recorded during the lifetime of the DEMETER mission were included in the present study; i.e. from September 2004 to December 2010.

We tried to identify and remove all of the time intervals when the data might be corrupted. We used a list of the single event upset events [Ziegler and Lanford 1979], which is available on the project website (http://demeter.cnrs-orleans.fr). The single event upsets are the results of effects on the microelectronic device (e.g. memory) of electromagnetic radiation caused by, e.g., an energetic particle. This can cause a change in state that occurs in or close to an important node of a logic element, which can consequently destroy the data measured at that given time. Moreover, we excluded the time intervals with possible non-natural events; e.g. interference of the Langmuir probe, monochromatic radiation, and diffusive noise, among others. A complete list of these events, along with their descriptions and examples, can be obtained from the website of the LPC2E laboratory in Orléans, France (ftp://lpc2e.cnrs-orleans.fr/projects/demeter/pub/SETI/).

For the earthquake data, we used the US Geological Survey earthquake catalog (http://earthquake.usgs.gov). Altogether, about 9,000 earthquakes with magnitudes ≥5.0 and depths ≤40 km occurred all over the world during the period analyzed. All of these were included in the study.

3. Processing methodology

We used the data processing method developed and described by Němec et al. [2008, 2009]. As the method is described in detail in these studies, we will only present a brief overview. The basic idea of the method is to collect all of the available data observed in the vicinity of earthquakes and to interpret these in the context of long-term distributions obtained for similar ionospheric conditions. In the first step of the data processing, it is therefore necessary to describe the distribution of the intensity of electromagnetic waves observed by DEMETER using all of the available data. This long-term distribution of intensities is calculated separately for each combination of the parameters used to characterize the state of the ionosphere. The parameters that we selected and the number of bins used for each of these are the same as those used by Němec et al. [2008], namely: frequency (16), geomagnetic latitude (66), geomagnetic longitude (36), magnetic local time (2), geomagnetic activity expressed by Kp index (3), and season of the year (2). We constructed a multidimensional array with the number of dimensions equal to the number of parameters. In each bin of this array, we stored a histogram of the wave intensities observed during the appropriate ionospheric conditions. The histograms were then used to construct the experimental cumulative distribution function (CDF) of the wave intensity for each of the bins.

In the second step of the data processing, the data related to the earthquakes (i.e. the data acquired close to earthquake epicenters both in space and time) are considered. These data were evaluated using the CDFs obtained in the first step of the data processing, and it was determined whether they were different from the expected distributions that were or were not seismically perturbed. To do so, we organized the data related to earthquakes into a grid, as a function of the frequency, the time relative to the main shock, and the distance from the epicenter. Moreover, the day-time and the night-time data were treated separately. Values that would be used more than once (typically the main shock and aftershocks) were excluded from our

analysis, to avoid the mixing of pre-seismic and post-seismic activity. Otherwise, a single measurement can be used more than once, and it would be impossible say to which earthquake the observed data can be attributed. This would result in greater uncertainty of the statistics.

For each measurement, the values of the corresponding CDF were evaluated. Afterwards, we calculate the mean values of the CDFs in each bin of the grid (the 'probabilistic intensity'; 0.5 is subtracted to get the mean value equal to 0). The resulting mean values were then normalized to have the mean value equal to 0 and the standard deviation equal to 1 (the 'normalized probabilistic intensity'). A lower estimate of the standard deviation used for normalization was obtained by taking into account the uniform distribution of the probabilistic intensity values, and by assuming that all of these values are independent. As this is not exactly the case, an additional factor is introduced, expressing the relative fraction of the data that was measured during the same half-orbit that can be considered as independent [see Němec et al. 2008, 2009].

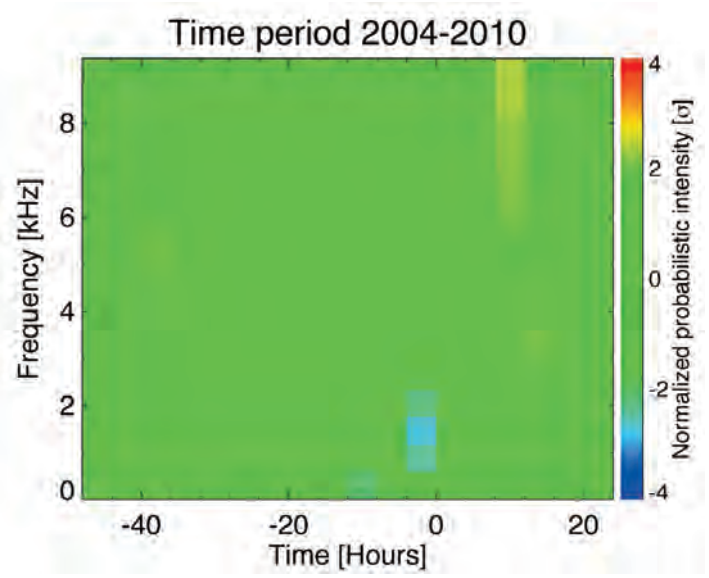

Figure 1. Frequency-time dependence of the normalized probabilistic intensity (see text) obtained from the night-time electric field data measured within 330 km from the epicenters of earthquakes with magnitudes ≥5.0 and depth ≤40 km.

4. Results

The main purpose of the present study is to apply the method of Němec et al. [2008] to the whole dataset acquired by the DEMETER satellite, and to determine whether the results obtained by Němec et al. [2008] using the first few years of data hold. To enable a direct comparison with the previously obtained results, exactly the same data processing method was used, with the same selection of frequency intervals and binning of individual parameters. Following their results, we have focused only on the night-time measurements in the vicinity of earthquakes with magnitudes ≥5.0 and with shallow depths ≤40 km.

Figure 1 shows the frequency-time dependence of the normalized probabilistic intensity obtained for distances lower than 330 km from the epicenter. It can be seen that the main observed feature is a decrease in the normalized probabilistic intensity at the frequency of about 1.7 kHz shortly before (0-4 h) the time of the main shocks. The value of this decrease corresponds to about 2.74 standard deviations. This effect is based on 3,920 values of CDFs collected during 115 different orbits. The mean value of the CDFs in this bin is about 0.419, which corresponds to a decrease in the wave intensity equal to about 2 dB. The night-time data in the frequency band centered at 1.7 kHz measured all over the world during all of the period analyzed were used as the referent distribution of wave intensities for the calculation of decreases in dB [see Němec et al. 2009, Figure A1]. From the same histogram, variations corresponding to one standard deviation from the mean are equal to about ± 7.5 dB.

Figure 2 shows the same dependence obtained for distances up to 440 km from the epicenter of earthquakes. The statistical significance of the effect is stronger when this

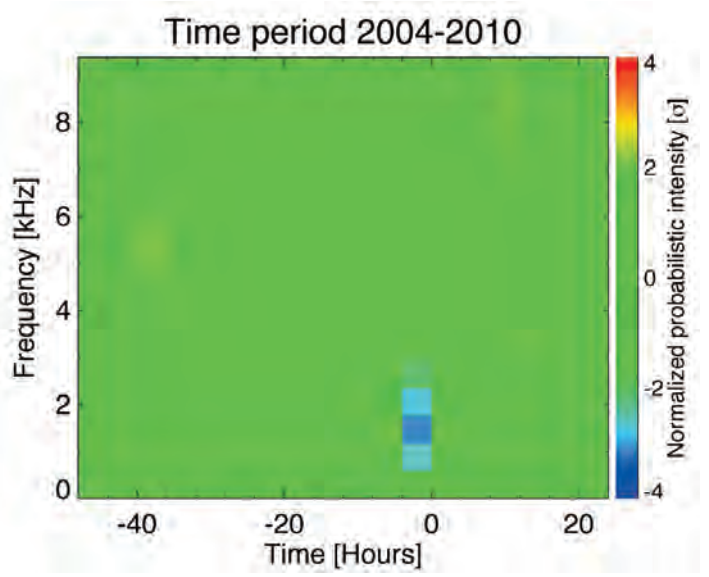

Figure 2. Frequency-time dependence of the normalized probabilistic intensity (see text) obtained from the night-time electric field data measured within 440 km from the epicenters of earthquakes with magnitudes ≥5.0 and depth ≤40 km.

extended area is considered. The normalized probabilistic intensity decreases by about 3 standard deviations. This effect is based on 6,790 values of CDFs collected during 153 different orbits. The mean value of the CDFs in this bin is 0.429, corresponding to a decrease in the wave intensity of about 1.8 dB.

Figure 3 shows the distance-time dependence of the normalized probabilistic intensity in the frequency interval 1,640 Hz to 1,740 Hz. This shows that the affected area is limited to distances ≤440 km from the epicenter. The effect

in this plot appears to be stronger at greater distances from the epicenter. However, as the amount of data included in the individual bins is not constant, but increases with the distance from the epicenter, a certain awareness is needed when interpreting the normalized results. The idea becomes clear when it is considered that even relatively small changes in the wave intensity can be statistically significant if they appear systematically in the large amount of data. On the other hand, even rather huge decreases in wave intensity would not be statistically significant if they were observed only in a couple of orbits. That this intuitive explanation is valid for our situation is demonstrated in Figure 4. This

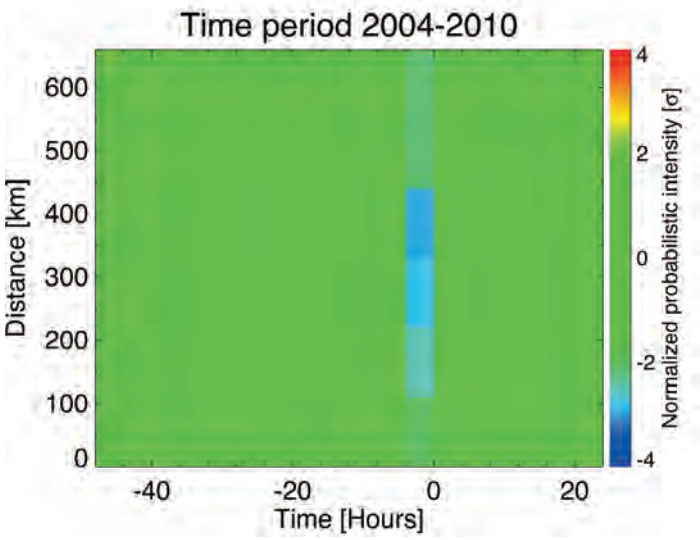

Figure 3. Distance-time dependence of the normalized probabilistic intensity (see text) obtained from the night-time electric field data measured at a frequency of about 1.7 kHz close to earthquakes with magnitude ≥5.0 and depth ≤40 km.

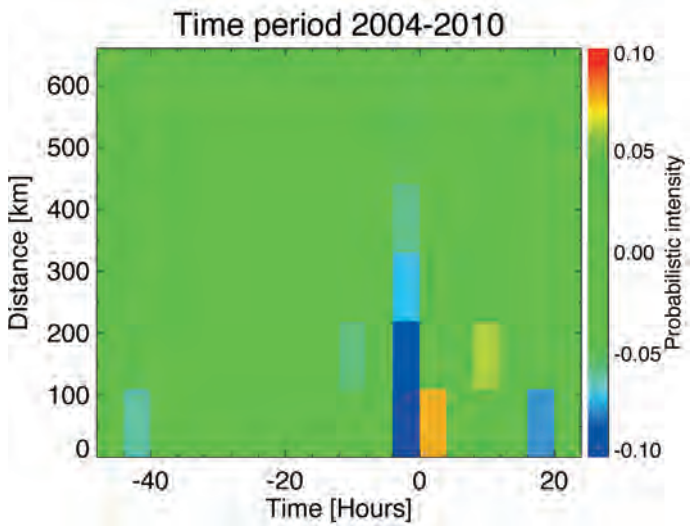

Figure 4. Distance-time dependence of the probabilistic intensity (without normalization; see text) obtained for the night-time electric field data measured at a frequency of about 1.7 kHz close to earthquakes with magnitude ≥5.0 and depth ≤40 km.

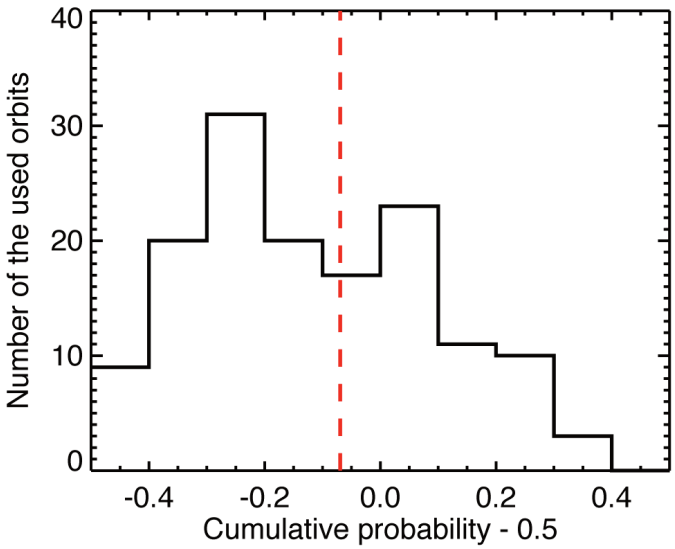

Figure 5. Distribution of the mean values of the CDFs that contribute to the observed wave intensity decrease. Vertical dashed red line, mean CDF.

represents the same dependence as in Figure 3, but this time for the results before the normalization; i.e. the values of the probabilistic intensity. It can be seen that the largest decrease in the probabilistic intensity is observed at distances <110 km from the epicenter, and the magnitude of the effect gradually decreases with increasing distance. It can be seen that an increase is clearly seen right after the time of the shocks. This is not a surprise, as it is known that the shock itself induces acoustic gravity waves that propagate upward [see for example, Blanc 1985].

To analyze the frequency-time interval that corresponds to the decrease in Figure 2 in more detail (i.e. the frequency range 1640 Hz to 1740 Hz, and the time interval 0 h to 4 h before the time of the main shock), we analyzed the distribution of the appropriate values of CDFs. Only the orbits with at least 12 values contributing to the effects were selected. A single value was obtained for each of these as a mean of the 12 CDF values closest to the epicenter. This was done as the data recorded within one orbit cannot be considered as independent. Using this procedure, we obtained a number of values that are lower than the number of orbits that contributed to the decrease in Figure 2. A histogram of these values is shown in Figure 5. It can be seen that this histogram is shifted towards the lower values, which corresponds to a decrease in the normalized probabilistic intensity. The mean value of the distribution is marked by the vertical dashed red line in Figure 5, which is about –0.069. We can evaluate the statistical significance of this shift; i.e. we can determine the probability that it might occur randomly. Two different methods were used. First, we used the classical t-test [Press et al. 1992, Ch. 14.2]. This is a statistical hypothesis test designed to assess whether the means of two normally distributed populations are equal. We have tested the

possibility that the observed deviation of the mean from 0 is random (0 is the expected mean if no seismic-related effects were present). The resulting probability is about 0.1%, which means that the observed deviation of the mean value from 0 is unlikely to be random. The second method that we used to estimate the statistical significance of the effects was to determine the number of values corresponding to the decrease (97) and the number of values corresponding to the increase (47). The probability that such a situation might occur randomly was then evaluated based on the binomial distribution with the anticipated probability of a decrease being equal to the anticipated probability of an increase. The resulting probability is lower than 0.1%, which means again that the observed shift toward the lower values is unlikely to be random.

5. Discussion

The existence of the previously reported decrease in the wave intensity shortly before the time of main earthquake shocks [Němec et al. 2008, 2009] has been confirmed here using the complete DEMETER dataset. However, the amplitudes of the observed effect – with mean and median CDFs of 0.419 and 0.375, respectively – are approximately the same as those reported in these previous studies. They reported mean and median CDFs as 0.417 and 0.374, respectively [Němec et al. 2009], and 0.354 and 0.324, respectively [Němec et al. 2008]. The differences might be caused by using different emission maps describing a longer time period. These can hide possible small time-scale effects, which can have a role in the final results.

It can be expected that any potential effect should be very close to the epicenter. However, Němec et al. [2009] showed a shift of the effect by 2 degrees westwards. This is not shown by our study, as we used a different analysis method than Němec et al. [2009]. We cannot therefore exclude that a small shift in the affected area from the vertical projection of the epicenter is hidden in statistical fluctuations of the results shown in Figure 4. This is also suggested by the normalized values shown in Figure 3.

The distribution of the mean values of the CDFs obtained for the data forming the effect shown in Figure 5 represents an independent test of the statistical significance of the effect. Moreover, it can be used to exclude the possibility that the decrease is caused by a few orbits of exceptionally low wave intensity. We used two independent statistical tests. The one sample t-test is designed specifically to test if a mean of a distribution is equal to a given value or not. However, it assumes that the distribution is normal, which is not exactly the case for the distribution studied here. Consequently, we used the independent and rougher test based on the binomial distribution. According to both of these tests applied, the decrease is statistically very significant.

As noted by Němec et al. [2008], the frequency of about 1.7 kHz where the decrease is observed corresponds approximately to the cut-off frequency of the Earth-ionosphere waveguide during the night-time [Budden 1961]. The lower frequency cut-off of this waveguide is inversely proportional to the height of the ionosphere. Taking into account that during the night-time the electromagnetic waves generated due to thunderstorm activity were a crucial source of VLF radiation observed by DEMETER [Němec et al. 2010], it can be expected that the exact frequency of this cut-off can significantly affect the power spectrum of the electromagnetic waves observed by DEMETER at frequencies close to 1.7 kHz. This is illustrated well in Figure 6, which presents an example of the frequency-time spectrogram of the power spectral densities of electric field fluctuations observed during one half orbit. The frequency cut-off at a frequency of about 1.7 kHz can be clearly identified as the frequency below which the power spectral density of the electric field fluctuations decreases drastically.

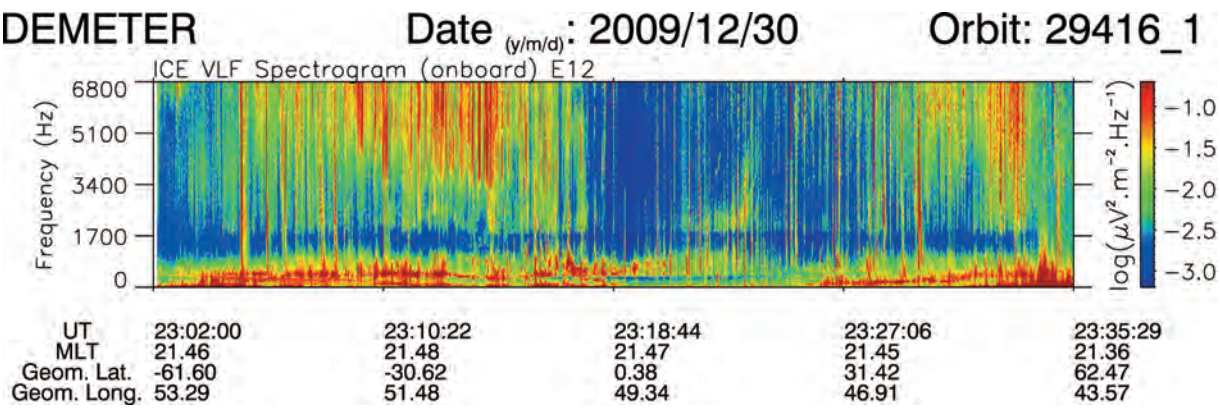

Figure 6. Frequency-time spectrogram of the power spectral density of the electric field fluctuations recorded by DEMETER along a complete half-orbit on December 30, 2009. Note the clear cut-off frequency of the whistlers (vertical lines) at about 1,700 Hz. The cut-off frequency remains relatively constant over all of the sampled latitudes.

An increase in this cut-off frequency would therefore necessarily lead to a decrease in the power spectral density of electric field fluctuations observed by DEMETER in the appropriate frequency range. Such an increase of the cut-off frequency would correspond to a decrease in the height of the ionosphere. Our results could therefore indicate that the height of the ionosphere is statistically lower above epicenters of imminent earthquakes. We have visually checked the earthquake orbits for the presence of such changes in the cut-off frequency. However, no clear change in the cut-off frequency was identified. This might be explained by the fluctuations of the background intensity in the dynamic range of about ±7.5 dB, as compared to the 2 dB change that corresponds to the attenuation effect. A more detailed analysis of the changes in the cut-off frequencies is beyond the scope of the present study, and this will be investigated in the future. According to a recent study by Harrison et al. [2010], this effect might result from an increase in the electric conductivity in the lower troposphere due to an increase in radon emanation prior to major earthquakes. The corresponding variations in the vertical atmospheric current that flows between the ionosphere and the surface of the Earth would modify the lower D-region electron density profile, and then the cut-off frequency of the Earth–ionosphere waveguide.

6. Conclusions

We have studied previously reported decreases in the intensities of electromagnetic waves at frequencies of about 1.7 kHz observed in the vicinity of imminent earthquakes [Němec et al. 2008, 2009]. Using the very large DEMETER dataset of ~6.5 years of measurements, we have confirmed that during the night there was a very small, but statistically significant, decrease in the wave intensity observed by the satellite close to earthquakes with magnitudes >=5.0 and depths <= 40 km shortly before the time of the main shocks (0-4 h). However, it is important to note that this effect is very small (a decrease of ~2 dB) as compared to the usual variations in the background activity (± 7.5 dB), and therefore it is very difficult to observe it directly in separate cases. These results are in agreement with an explanation suggested by Harrison et al. [2010] based on changing the properties of the Earth-ionosphere waveguide. Attenuation of a certain type of waves (e.g. 0+ whistlers) has not been visually detected.

Acknowledgements. This study was supported by the Centre National d'Etudes Spatiales. It is based on observations with the electric field experiment embarked on DEMETER. The authors thank J.J. Berthelier, the PI of this instrument, for the data supply. A part of the studies leading to these results was also funded from the European Community Seventh Framework Programme (FP7/2007-2013), under grant agreement n° 262005. We acknowledge additional support from grants ME09107, GACR 205-09-1253, and GAUK 403511.

References

Asada, T., H. Baba, M. Kawazoe and M. Sugiura (2001). An attempt to delineate very low frequency electromagnetic signals associated with earthquakes, Earth Planet. Space, *53*, 55-62.

Berthelier, J.J., M. Godefroy, F. Leblanc, M. Malingre, M. Menvielle, D. Lagoutte, J.Y. Brochot, F. Colin, F. Elie, C. Legendre, P. Zamora, D. Benoist, Y. Chapuis and J. Artru (2006). ICE, the electric field experiment on DEMETER, Planet. Space Sci., *54*, 456-471.

Blanc, E. (1985). Observations in the upper atmosphere of infrasonic waves from natural or artificial sources: a summary, Ann. Geophysicae, *3*, 673-688.

Bortnik, J., J.W. Cutler, C. Dunson and T.E. Bleier (2008). The possible statistical relation of Pc1 pulsations to earthquake occurrence at low latitudes, Ann. Geophys., *26*, 2825-2836.

Budden, K.G. (1961). The Waveguide Mode Theory of Wave Propagation, London, Logos Press; Englewood Cliffs, N.J., Prentice-Hall [c1961].

Clilverd, M.A., C.J. Rodger and N.R. Thomson (1999). Investigating seismoionospheric effects on a long subionospheric path, J. Geophys. Res., 104, 28171-28179.

Freund, F.T. (2007). Pre-earthquake signals: part 1. Deviatoric stresses turn rocks into a source of electric currents, Nat. Haz. Earth Syst. Sci., *7*, 535-541.

Freund, F. (2011). Pre-earthquake signals: Underlying physical processes, Original Research Article, J. Asian Earth Sci., *41*, 383-400.

Gershenzon, N.I., M.B. Gokhberg, A.V. Karakin, N.V. Petviashvili and A.L. Rykunov (1989). Modelling the connection between earthquake preparation processes and crustal electromagnetic emission, Phys. Earth Planet. Inter., *57*, 129-138.

Harrison, R.G., K.L. Aplin and M.J. Rycroft (2010). Atmospheric electricity coupling between earthquake regions and the ionosphere, J. Atmos. Sol. Terr.. Phys., *72*, 376-381.

Henderson, T.R., V.S. Sonwalkar, R.A. Helliwell, U.S. Inan and A.C. Fraser-Smith (1993). A search for ELF/VLF emissions induced by earthquakes as observed in the ionosphere by the DE 2 satellite, J. Geophys. Res., 98, 9503-9514.

Hobara, Y., F. Lefeuvre, M. Parrot and O.A. Molchanov (2005). Low-latitude ionospheric turbulence observed by Aureol-3 satellite, Ann. Geophys., *23*, 1259-1270.

Larkina, V.I., V.V. Migulin, O.A. Molchanov, I.P. Kharkov, A.S. Inchin and V.B. Schvetcova (1989). Some statistical results on very low frequency radiowave emissions in the upper ionosphere over earthquake zones, Phys. Earth Planet. Inter., *57*, 100-109.

Molchanov, O.A. and M. Hayakawa (1998). On the generation mechanism of ULF seismogenic electromagnetic emissions, Phys. Earth Planet. Inter., 105, 201-210.

Molchanov, O.A., O.A. Mazhaeva, A.N. Goliavin and M.

Hayakawa (1993). Observation by the Intercosmos-24 satellite of ELF-VLF electromagnetic emissions associated with earthquakes, Ann. Geophys., 11, 431-440.

Molchanov, O., A. Rozhnoi, M. Solovieva, O. Akentieva, J. J. Berthelier, M. Parrot, F. Lefeuvre, P.F. Biagi, L. Castellana and M. Hayakawa (2006). Global diagnostics of the ionospheric perturbations related to the seismic activity using the VLF radio signals collected on the DEMETER satellite, Nat. Haz. Earth Syst. Sci., 6, 745-753.

Němec, F., O. Santolík, M. Parrot and J.J. Berthelier (2008). Spacecraft observations of electromagnetic perturbations connected with seismic activity, Geophys. Res. Lett., 35, L05109; doi: 10.1029/2007GL032517.

Němec, F., O. Santolík and M. Parrot (2009). Decrease of intensity of ELF/VLF waves observed in the upper ionosphere close to earthquakes: A statistical study, J. Geophys. Res., 114, A04303; doi: 10.1029/2008JA013972.

Němec, F., O. Santolík, M. Parrot and C.J. Rodger (2010). Relationship between median intensities of electromagnetic emissions in the VLF range and lightning activity, J. Geophys. Res., 115, A08315; doi: 10.1029/2010JA015296.

Parrot, M. and M.M. Mogilevsky (1989). VLF emissions associated with earthquakes and observed in the ionosphere and the magnetosphere, Phys. Earth Planet. Inter., 57, 86-99.

Parrot, M. (1994). Statistical study of ELF/VLF emissions recorded by a low-altitude satellite during seismic events, J. Geophys. Res., 99, 23339-23347.

Parrot, M. (Ed.) (2006). First results of the DEMETER microsatellite, Special Issue of Planet. Space Sci., 54, 411-558.

Press, W.H., S.A. Teukolsky, W.T. Vetterling and B.P. Flannery (1992). Numerical Recipes in C. The Art of Scientific Computing, 2nd Edition, Chapter 14.2.

Rodger, C.J., N.R. Thomson and R.L. Dowden (1996). A search for ELF/VLF activity associated with earthquakes using ISIS satellite data, J. Geophys. Res., 101, 13369-13378.

Serebryakova, O.N., S.V. Bilichenko, V.M. Chmyrev, M. Parrot, L. Rauch, F. Lefeuvre and O.A. Pokhotelov (1992). Electrodynamic ELF radiation from earthquake regions as observed by low-altitude satellites, Geophys. Res. Lett., 19, 91-94.

Sorokin, V.M., V.M. Chmyrev and A.K. Yaschenko (2001). Electrodynamic model of the lower atmosphere and the ionosphere coupling, J. Atmos. Sol. Terr. Phys., 63, 1681-1691.

Tate, J. and W. Daily (1989). Evidence of electro-seismic phenomena, Phys. Earth Planet. Inter., 57, 1-10.

Ziegler, J.F. and W.A. Lanford (1979). Effect of cosmic rays on computer memories, Science, 206, 776-788.

*Corresponding author: David Píša
Institute of Atmospheric Physics, Academy of Science of the Czech Republic, Prague, Czech Republic;
e-mail: david.pisa@cnrs-orleans.fr